THE AMERICAN SOCIETY OF MECHANICAL ENGINEERS
345 E. 47th St., New York, N.Y. 10017

96-GT-478

An Unsteady Velocity Formulation for the Edge of the Near-Wall Region

Dennis E. Wilson
Anthony J. Hanford
Department of Mechanical Engineering
The University of Texas at Austin

ABSTRACT

A phenomenological model is presented that relates freestream turbulence to the augmentation of stagnation-point surface flux quantities. The model requires the turbulence intensity, the longitudinal scale of the turbulence, and the energy spectra as inputs for the unsteady velocity at the edge of the near-wall viscous region. The form of the edge velocity contains both pulsations of the incoming flow and oscillations of the streamline.

Incompressible results using a single fluctuating component are presented within the stagnation region of a two-dimensional cylinder. The time-averaged Froessling number is determined from the computations. These predictions are compared to existing incompressible experimental data. Additionally, the variations in the surface flux quantities with the longitudinal scale of the incoming freestream turbulence, the Reynolds number, and the freestream turbulence intensity are considered.

NOMENCLATURE

Variables and Symbols

a_n	Pulsation parameter for frequency n.
b^*	An appropriate length scale equivalent tothe half width of the stagnation region. [*meters*]
b_n^*	Oscillation parameter for frequency m. [*meters*]
c^*	Inviscid strain rate (Hiemenz parameter). [*per second*]
C_H	The strain rate constant with a value of 3.7.
D^*	Characteristic length on the bluff body. For a circular cylinder this is the diameter. [*meters*]
$E^*(\kappa^*,t^*)$	Three-dimensional energy-spectrum function for the turbulence. [*cubic meters per seconds squared*]
e_n	Fluctuating energy at the frequency n compared to the total energy in the fluctuations. Summation of e_n^2 over the range from 1 to N is defined as unity.e_{on} e_n before normalization.
Iu,Iv	Turbulence intensities using only the fluctuations from the U^* component and V^* component, respectively.
k_t	The turbulent kinetic energy [*square meters per square seconds*]
N	Total number of frequencies for a_n and β_n, respectively.
Nu_D	Nusselt number based on the characteristic body length, D^*.
n	Nondimensional integral frequency.
$\hat{n}$	Nondimensional integral frequency at the midpoint of the range of the energy-containing eddies.
P^*,p^*	Pressure outside the near-wall viscous region and within the near-wall viscous region, respectively. [*Newtons per square meter*]
Re_D	Reynolds number based on the characteristic body length, D^*, and the mean freestream velocity and kinematic viscosity.
t^*	Time. The nondimensional time is $t=\Omega^* t^*$. [*seconds*]
Tu	Overall turbulence intensity. In this paper, Tu (without a subscript) is equivalent to Tu_∞.
U^*,u^*	Circumferential fluid velocities parallel to the body surface outside the near-wall viscous region and within the near-wall viscous region, respectively. The nondimensional velocity at the edge of the near-wall viscous region is $U_e=U_e^*/c^*b^*$. [*meters per second*]
V^*,v^*	Fluid velocities perpendicular to the body surface outside the near-wall viscous region and within the near-wall viscous region, respectively. The nondimensional velocity at the edge of the near-

Presented at the International Gas Turbine and Aeroengine Congress & Exhibition
Birmingham, UK — June 10-13, 1996
This paper has been accepted for publication in the Transactions of the ASME
Discussion of it will be accepted at ASME Headquarters until September 30, 1996

	wall viscous region is $v_e = v_e^* / \left(v_\infty^* c^*\right)^{1/2}$. [*meters per second*]
X^*, Y^*	Vertical and horizontal coordinates, respectively, using the cylinder centerline as the origin.
$x_p^{*'}$	Position of some particle p in terms of X^* due to the local velocity fluctuations.
x^*, y^*, z^*	Circumferential coordinate on the body surface measured from the mean forward stagnation line, the coordinate perpendicular to the body surface measured from the surface, and the axial or spanwise coordinate, respectively. The nondimensional coordinates are $x = x^*/b^*$ and $y = y^*\left(c^*/v_\infty^*\right)^{1/2}$. [*meters*]
Z_U, Z_V	Normalized fluctuation correlations for the $U^{*'}$ and $V^{*'}$ turbulence components, respectively.

Greek Symbol — Definition [*units*]

α_Ω	Nondimensional frequency.
β_n	Nondimensional oscillation parameter at frequency n, $\beta_n = b_n^*/b^*$.
β_{01}, β_{02}	Constants in the definition of the oscillation parameter.
δ_e^*	Thickness of the near-wall viscous region. [*meters*]
κ^*	Wave number of the turbulence fluctuation. [*per meter*]
$\hat{\kappa}^*$	Wave number at the center of the range of the energy containing eddies. [*per meter*]
λ^*	Longitudinal integral length of scale turbulence. The nondimensional integral length scale is $\lambda = \lambda_\infty^*/D^*$ [*meters*]
λ_{1U}	Value of λ for Z_{1U}.
λ_{1V}	Nondimensional transverse integral length scale for Z_{1V}.
ν^*	Kinematic viscosity. [*square meters per second*]
ρ^*	Density. Nondimensional density is $\rho = \rho^*/\rho_\infty^*$. [*kilograms per cubic meter*]
Ω^*	Characteristic frequency of the large-scale, freestream unsteadiness. [*radians per second*]
Ω_n^*	Characteristic frequency at frequency n, $\Omega_n^* = n\,\Omega^*$.

Superscripts and Overbars

*	A dimensional quantity. Nondimensional quantities do not carry a '*'.
'	A fluctuating quantity when placed on a velocity.
overbar	A time-independent or mean quantity.
$\lvert\ \rvert$	Magnitude of the quantity within.

Subscripts

e	A quantity evaluated at the edge of the near-wall viscous region.
n	A quantity at frequency n.
t	Quantity defined using a turbulent model
w	A quantity evaluated at the wall.
∞	A quantity evaluated at a position on the mean stagnation streamline just upstream of the region influenced by the body in the flow. For a supersonic case, this position is downstream from any shock.

INTRODUCTION

In general the flow inside a gas turbine is three-dimensional and highly unsteady. The unsteadiness arises from several sources including secondary flow vortices, shock wave passing, periodic variations in the potential flow, and wake passing. It is this last source of flow unsteadiness which has attracted the most attention. The wakes form behind upstream blades and convect downstream and impinge upon other rotor blades. These wakes produce an incident flow which is periodically unsteady in the mean velocity and contains a relatively high turbulence level. This highly turbulent, impinging wake flow significantly alters the boundary layer around the rotor blade. The two effects which are most important here are wake-induced transition on the suction surface and heat transfer augmentation in the stagnation region. It is this second effect which motivated the development of the unsteady edge model described in this paper.

The leading edge of a gas turbine airfoil represents a stagnation region with a highly unsteady (turbulent) freestream. The highest heat transfer rate is usually measured in this region even when the freestream is laminar or has a low level of turbulence. For a highly turbulent freestream the heat transfer can increase by a factor of 1.5 or 2.0. This phenomena is of considerable importance in the gas turbine community for two basic reasons. First, an accurate prediction of heat transfer rates is a major design consideration. Second, the mechanism by which freestream turbulence alters heat and momentum transfer within the stagnation point boundary layer is not completely understood.

The ultimate objective of this research is to develop a model which predicts enhanced stagnation region heat transfer associated with wake-generated freestream turbulence within gas turbines. This study considers only the effect of freestream turbulence. The relative motion and unsteady mean flow effects inherent in gas turbines are ignored in this initial formulation. Dullenkopf and Mayle (1994) have, however, developed correlations which consider both incident turbulence and moving wake effects.

The model described in this paper is intended to represent how organized vorticity patterns generally referred to as coherent structures alter the stagnation region boundary layer. These coherent structures can be generated by a number of well-known mechanisms. Examples of generating devices include rotor blades, turbulence grids, two-dimensional cylinders, splitter plates, and free jets. The structures produced downstream of a circular cylinder due to vortex shedding have vorticity of alternating sign. If the freestream turbulence is produced by a splitter plate with two streams of differing velocity, large scale coherent structures of the same sign are produced. The approach adopted in this paper has two advantages. First, by eliminating the extraneous complications of the freestream, a model is developed which provides some fundamental insight into the mechanisms by which organized vorticity fluctuations alter the heat and momentum transfer inside a

boundary layer. Second, a considerable experimental data base exists for relatively well-defined freestream turbulent flows. The key features these vorticity patterns have in common which are important to the present unsteady velocity model are:

- The coherent structures are quasi-two-dimensional and the unsteadiness is quasi-periodic.
- The unsteady energy is confined to a narrow spectrum allowing its behavior to be captured by only a few frequencies or length scales.
- The vorticity axis is aligned parallel to the major axis of the downstream body which can be represented as a cylinder.

Furthermore, we represent the effect of these unsteady structures upon the stagnation region boundary layer as a fluctuation of the stagnation point streamline and a pulsation of the incoming flow. And finally, we assume that the role of these structures on the stagnation region is to modify the time averaged pressure gradient and velocity at the edge of the boundary layer.

STAGNATION POINT HEAT TRANSFER

Laminar stagnation point theory has been successfully used to predict the heat flux when the flow conditions meet the restrictions built into the model; that is, the freestream must be laminar or at least have turbulence intensities no higher than approximately one percent

When the flow field departs from these almost ideal conditions, the agreement between theory and experiment diverges. In particular, when spatial and temporal fluctuations are introduced into the freestream, the heat and momentum transfer in the boundary layer can become significantly enhanced. These fluctuations are commonly referred to as freestream turbulence, and the phenomena are called *freestream turbulence effects*. This notation is misleading since the fluctuations can be either vortical (turbulence) or potential (irrotational). The disunction is more than semantics, because both types of fluctuation can lead to enhanced heat and momentum transfer.

Experiments

Surface heat transfer can be correlated using the Froessling number, F_s, defined as

$$F_s \equiv \frac{Nu_D}{Re_D^{1/2}\, Pr^m}$$

where the exponent, m, varies between 0.33 and 0.40. For most experiments, the Prandtl number is constant and the Froessling number is shortened to $Nu\, Re_D^{-1/2}$.

Hanford (1994) conducted an extensive review of experimental studies which measured the augmentation of stagnation-point surface fluxes due to turbulence generated upstream of a circular cylinder. In most of the experiments, the cylinder is placed completely across the test section. Artificially high levels of turbulence are generated upstream of the test cylinder within shear layers formed behind screens. Screens with a rectangular mesh generate shear layer vorticity oriented along both major axes of a tunnel's cross section. Screens composed of parallel rods produce vorticity again oriented along both major axes of a tunnel's cross section. However, the vorticity component parallel to the rods is stronger than its perpendicular counterpart. The rods, and thus the stronger component of generated vorticity, may be parallel to or perpendicular to the test cylinder. The generated turbulence is greatest just downstream of the screen, decaying with distance. Further, most researchers prefer that the turbulence impinging upon the test model be homogeneous. Screen generated turbulence is nonhomogeneous for some distance from its origin, which is a function of the mesh geometry. As such, the proximity of the model to the turbulence generator is limited by these considerations. The turbulence which reaches the test cylinder and, therefore, the heat transfer augmentation, is a complex function of the tunnel geometry and other attributes of the flow.

Researchers have also collected data on the augmentation of surface mass transfer due to freestream turbulence. In these studies a sublimating solid replaces the thermocouples or heat flux gages employed in heat transfer studies. Further, mass transfer studies naturally supply a constant concentration condition at the surface which is equivalent to a constant temperature condition in heat transfer studies. Theoretically, the two types of studies may be related to each other through the Reynolds analogy for heat and mass transfer. However, this approach introduces additional uncertainties which may be significant.

Data from fourteen of these studies are displayed in Figures 1 and 2. Data sets from studies which contained large experimental uncertainties and data taken at Reynolds numbers below 17,000 were excluded. Three curves are also included in these figures. The first is the phenomenological model developed by Smith and Kuethe (1966) for a Reynolds number of 100,000. The other two curves are empirical parabolic fits to the data of Kestin and Wood (1971), and Lower and Vachon (1975). Froessling calculated a limiting theoretical value for $Nu_D / Re_D^{1/2}$ of 0.945 at a turbulence intensity of zero. The existing experimental results do not collapse to a single curve when correlating $Nu_D / Re_D^{1/2}$ as a function of $Tu_D\, Re_D^{1/2}$ alone.

Hanford (1994) reviewed these studies in detail and summarized several consensus findings. The conclusions which are pertinent to the model derived in this paper are given below.

- Four parameters are recognized by current researchers as being suitable for correlating local heat transfer augmentation due to freestream unsteadiness. These parameters are Nusselt number, Reynolds number, freestream turbulence intensity, and the nondimensional turbulence scale.
- Surface heat transfer increases for increases in either Reynolds number or turbulence intensity.
- Heat transfer is a maximum when $\left(\lambda_\infty^* / D^*\right) Re_D^{1/2}$ is approximately 10.
- Either turbulence parameter, $TuRe_D$ or $TuRe_D^{1/2}$, does equally well collapsing heat transfer data (Dyban, Epick, and Kozlova, 1974). Because neither parameter includes the nondimensional scale of the freestream turbulence they can be used for correlating data only when the variations in the nondimensional scale of turbulence are small (Ames and Moffat, 1990).
- Recently Dullenkopf and Mayle (1995) proposed a new turbulence parameter which accounts for both turbulence intensity and length scale. This parameter which leads to a simple heat transfer correlation is related to the pulsation parameter in the unsteady velocity model.

Theory

Attempts at modeling the effect of freestream turbulence in the stagnation region have been largely unsuccessful primarily because of a misunderstanding of the physical mechanisms. Many researchers have attempted to "force" turbulence into laminar stagnation point theories by simply adding a turbulence transport term into the time-averaged equations. However, most boundary layers are not fully turbulent at the stagnation region and, prior to transition, they are pseudo-laminar and unsteady (Taulbee and Tran, 1988). Or, as Hoshizaki, Chou, Kulgein, and Meyer (1975) state, "There seems to be no evidence from [experimental] results that the effect of free stream turbulence is to trip the laminar boundary layer and make it turbulent. Rather, the transport in the usual laminar boundary layer seems to be augmented."

Outside the boundary layer, both vortical (turbulence) and potential fluctuations do exist; however, their effect is felt inside the boundary layer in a manner which cannot be satisfactorily modeled by the inclusion of a classic turbulence transport term. When the fluctuations are vortical, the physical mechanism which alters the velocity and temperature profiles is primarily a modification of the time-averaged pressure gradient and boundary-layer edge condition. Hoshizaki, Chou, Kulgein, and Meyer (1975), also note that, "... most of the boundary layer is dominated by viscous forces and that turbulence represents an additional 'outer flow' transport term which steepens the relevant wall gradients."

A few researchers have solved the unsteady boundary-layer equations (Lighthill, 1954, Lin, 1957, and Ishigaki, 1970). Although the mathematical analysis is generally sound, most of these studies assume arbitrary periodic flows without attempting to relate the prescribed edge velocity to realistic freestream conditions. However, Lin (1957) did note a possible application of this work to the flow past turbine blades.

Several papers have appeared which specifically address how a particular freestream disturbance of engineering interest might alter the stagnation-point flow field. For example, Cebeci, Krainer, Simoneau, and Platzer (1987) modeled a freestream flow containing a wake passing perpendicular to the mean flow axis. Bogucz, Dirik, and Lyman (1988) considered an approaching flow which included a pair of counter-rotating vortices. Both of these studies reported significant unsteady components in the stagnation point velocity and temperature profiles. Paxson and Mayle (1991) represented the outer flow as a steady component, a periodic component from the passing wake, and a fluctuating component arising from the freestream turbulence. They concluded that the fluctuations in the freestream may be treated as essentially inviscid effects impressed upon the boundary layer. These investigations provide an understanding of how the spatial and temporal fluctuations of a freestream influence stagnation-region skin friction and heat transfer.

RESEARCH OBJECTIVE AND METHODOLOGY

This paper helps to quantify how wake generated freestream turbulence alters the wall flux quantities. This approach differs from previous studies in that it relates freestream parameters such as turbulence intensity, length scale, and energy spectra directly to the unsteady boundary layer equations.

To be useful as an engineering tool, a model must have two essential components. First, it must be relatively simple to use for a wide variety of flow field calculations. Second, the model must include the essential physics to be truly predictive. That is, it must not contain arbitrary parameters which are adjusted to accurately reproduce experimental data for some set of very specific flow conditions.

This paper presents a simple phenomenological model for the unsteady velocity at the edge of the boundary layer and then relates the characteristic freestream turbulence parameters to this boundary layer edge velocity. It should be emphasized that the edge velocity model represents a *manifestation* of the way in which freestream vorticity alters the boundary layer. In other words, it does not contain the time-dependent freestream vortical structures but models their *effect* insofar as the stagnation-point flow field is concerned. This simple vorticity model for the freestream turbulence does, however, characterize the turbulence intensity, length scale effect, and energy spectra. These parameters are then directly related to the velocity edge model.

The overall methodology may be summarized by the following points:

- Model the effect of the turbulence in the near-wall, viscous region using a fluctuating *edge velocity model* containing both a pulsation of the incoming flow and an oscillation of the instantaneous stagnation point.
- Characterize the freestream turbulence structure by a *simple vorticity model* using the parameters of turbulence intensity, energy spectra, and turbulent length scale.
- Characterize the distortion of the turbulence due to the strain field using Rapid Distortion Theory.
- Incorporate these effects into the boundary layer equations and solve both the unsteady and time averaged equations.

The unsteady velocity model is restricted to a specialized but quite common freestream turbulent flow. Specifically, the model applies to wake generated or free shear layer generated turbulence. Under these conditions, the turbulent structure is reasonably well-defined. In particular, the large-scale structures are assumed to be quasi-two-dimensional and quasi-periodic. This implies that the vorticity is predominately two-dimensional and only a few length scales are necessary to quantify the unsteady behavior. With these ideas in mind, the phenomenological edge model and the simple vorticity model are presented next.

The ultimate objective of this research is a numerical technique which accurately predicts the augmentation of surface flux quantities at the stagnation point of a blunt body for compressible freestream flows due to wake-induced fluctuations. This paper deals only with the formulation of the unsteady model. Details of the numerical solution of the mean and unsteady boundary layer equations for an incompressible flow are given by Hanford and Wilson (1994).

UNSTEADY VELOCITY MODEL FORMULATION

In previous work related to this research (Hanford and Wilson, 1994) a model for the fluctuating velocity at the edge of the near-wall viscous region was presented. This model contained the pulsation parameter, a_n, and the oscillation parameter, β_n. A crude model related the intensity of the freestream turbulence to a_n. The oscillation parameter was determined by matching the numerical simulations with experimental data at two values of

$Tu Re_D^{1/2}$. This section describes a simple vorticity model for the freestream turbulence which directly relates the parameters to the velocity edge model. The first subsection describes the velocity edge model and the second subsection develops the freestream vorticity model which quantifies a_n and β_n without the use of correlations or curve fits.

Phenomenological Edge Velocity Model

At the edge of the near-wall viscous region on the mean stagnation streamline, the flow may be described as quasi-laminar. Referring to Figure 3, the flow may be decomposed into a mean flow plus fluctuating components. These fluctuating components, without regard for their original source, will be felt at the edge of the near-wall viscous region as a series of pulsations along the mean stagnation line plus a series of oscillations about the mean stagnation line. For turbulent eddies there will be a distribution of cylindrical structures each rotating at some frequency which is characteristic of the eddy's size. The effect of this turbulence can be modeled by a finite number of cylindrical structures rotating at a finite number of discrete frequencies. This implies that the mean flow at the edge of the near-wall viscous region will contain an additional number of pulsations and a similar number of oscillations at some discrete frequencies.

On the basis of this model, the edge-velocity parallel to the wall can be written as the sum of the mean flow plus a finite number of pulsations and oscillations.

$$U_e^*\left(x^*,y^*,t^*\right)=c^*\left[1-\sum_{n=1}^{N}a_n\sin\left(\Omega_n^*t^*\right)\right]\left[x^*-\sum_{n=1}^{N}b_n^*\sin\left(\Omega_n^*t^*\right)\right] \tag{1}$$

The indicated series are summed from one to some finite value. The nondimensional amplitude, a_n, is the ratio of the fluctuating velocity to the average velocity in the inviscid flow at the edge of the near-wall viscous region. Thus, the first set of terms represents the pulsation of the incoming flow and a particular component, a_n, is equal to $\left|V_e^{*'}\right|/\bar{V}_e^*$. The dimensional parameter, b_n^*, represents the displacement amplitude of the incoming stagnation streamline. Consequently, this second set of terms represents the oscillation. The parameter c^* is the inviscid strain rate.

The above relationship assumes only N dominant frequencies are necessary to characterize the time dependence of the large-scale vortical structures. This is a valid assumption when the bulk of the fluctuating kinetic energy in the freestream unsteadiness falls in a narrow frequency band. Fluctuating energy spectra measurements in freestream turbulence (Britter, Hunt, and Mumford, 1979) and turbulent shear layers (Driver, Seegmiller, and Marvin, 1987) suggest this simplification to be valid.

An expression for the edge-velocity normal to the body surface may be developed based on equation (1) plus the continuity equation. The pulsating nature of the incoming flow is evident in the resulting equation.

$$V_e^*\left(x^*,y^*,t^*\right)=-c^*\left[1-\sum_{n=1}^{N}a_n\sin\left(\Omega_n^*t^*\right)\right]y^* \tag{2}$$

In nondimensional form, the two components of the edge velocity may be expressed as

$$U_e(x,t)=\left[1-\sum_{n=1}^{N}a_n sin(nt)\right]\left[x-\sum_{n=1}^{N}\beta_n sin(nt)\right] \tag{3 a}$$

$$V_e(y,t)=-\left[1-\sum_{n=1}^{N}a_n\sin(nt)\right]y \tag{3 b}$$

The corresponding pressure gradient becomes

$$\alpha_\Omega^2\frac{\partial U_e}{\partial t}+U_e\frac{\partial U_e}{\partial x}=-\frac{p_{scale}^*}{\rho_\infty^*\left(c^*b^*\right)^2}\frac{1}{\rho_e}\frac{\partial P_e}{\partial x} \tag{4}$$

Because the pressure distribution will be impressed upon the near-wall viscous region by the outer flow, equation (4) reduces the governing equations within the near-wall viscous region to a boundary layer formulation. The compressible and incompressible boundary layer equations use a different p_{scale}^*. For incompressible flow $p_{scale}^*=\rho_\infty^*\left(c^*b^*\right)^2$. The pressure gradient is set once a_n, β_n, and α_Ω are known. These parameters are presented below.

Vorticity Model

As illustrated in Figure 3, the fluctuations in the freestream may be modeled by a simple vorticity model superimposed upon a uniform mean flow. Here the coordinate system using capital letters, (X^*,Y^*), has its origin at the center of a two-dimensional circular cylinder of diameter D^*. A second coordinate system, (x^*,y^*), originates at the mean forward stagnation point with the coordinate x^* along the body surface in the circumferential direction. Referring to Figure 3, the fluctuating components for a single ideal vortex in the freestream may be expressed as

$$U^{*'}=\left|U_\infty^{*'}\right|sin\left[\frac{2\pi}{\lambda_\infty^*}\left(Y^*-V_\infty^*t^*\right)\right] \tag{5 a}$$

$$V^{*'}=\left|V_\infty^{*'}\right|sin\left[\frac{2\pi}{\lambda_\infty^*}\left(X^*-V_\infty^*t^*\right)\right] \tag{5 b}$$

In general equation set (5) applies at any point along the stagnation streamline. The X^* position of a particle p at any location as a function of time can be found by noting that $U^{*'}=dX_p^{*'}/dt^*$ and integrating equation(5 a).

$$X_p^{*'} = \frac{\lambda^*}{2\pi}\frac{|U^{*'}|}{V^*}\cos\left[\frac{2\pi}{\lambda^*}\left(Y^* - V^* t^*\right)\right] + \text{constant}$$

Taking the integration constant as zero, the amplitude, $|X_p^{*'}|$, can be written as

$$|X_p^{*'}| = \frac{\lambda^*}{2\pi}\frac{|U^{*'}|}{V^*} = \frac{\lambda^*}{2\pi}\left|\frac{U^{*'}}{U_\infty^{*'}}\right|\frac{|U_\infty^{*'}|}{\overline{V}_\infty^*}\frac{\overline{V}_\infty^*}{V^*} \qquad (6)$$

where $V^* = \overline{V}^* + |V^{*'}|$. The components of the turbulence intensity at some station 'i' and the instantaneous velocity are defined as

$$Iu_i = \frac{|U_i^{*'}|}{\overline{V}_i^*} \qquad Iv_i = \frac{|V_i^{*'}|}{\overline{V}_i^*} \qquad Tu_i^2 = \frac{Iu_i^2 + Iv_i^2}{2} \qquad (7)$$

In the definitions of turbulence intensity given by expression set (7), the magnitude of the mean velocity vector is the proper denominator for the first two equations. Away from the body, however, the magnitude of the mean velocity vector may be replaced by the mean uniform velocity, $\overline{V}_i^*$. Then, in terms of the definitions given in (15) $|X_p^{*'}|$ becomes

$$|X_p^{*'}| = \frac{\lambda^*}{2\pi}\left|\frac{U^{*'}}{U_\infty^{*'}}\right| Iu_\infty\left[\frac{\overline{V}^*}{\overline{V}_\infty^*} + Iv_\infty\frac{V^{*'}}{|V_\infty^{*'}|}\right]^{-1} \qquad (8)$$

Oscillation Parameter, β_n

To determine the oscillation parameter a working definition of the edge of the near-wall viscous region is necessary. A sketch of this region (shown in Figure 4) indicates the various length scales referred to in this analysis. For a laminar, or low turbulence freestream, the edge of the boundary layer is well defined. This relation is

$$\frac{\delta_e^*}{D^*} = \frac{2.4}{C_H^{1/2}}Re_D^{-1/2} \qquad (9)$$

Referring to Figure 4, we see that $\delta_e^* = 2.4\,\delta_H^*$ where δ_H^* is the (Hiemenz) viscous length scale. However, for a highly turbulent freestream the boundary layer the edge is more difficult to determine. Nevertheless, an expression is needed in order to proceed with this analysis. Based on the analysis of Taulbee and Tran (1988), the edge of the boundary layer, δ_e^*, is given by

$$\delta_e^* = 2.4\left(\nu_e^*/c^*\right)^{1/2} \qquad (10)$$

where $c^* = C_H\overline{V}_\infty^*/D^*$ and ν_e^* is the "effective" viscosity given by $\nu_e^* = \nu^* + \nu_t^*$. Taulbee and Tran (1899) define the turbulent eddy viscosity as $\nu_t^* = 0.09\,k_t^{1/2}\,\lambda_\infty^*$, where $k_t = 1.5\,(Tu_\infty\,\overline{V}_\infty^*)^2$. We have modified their expression by using an effective viscosity, whereas they use only the turbulent eddy viscosity in equation (10). Substituting these expressions into equation (10) yields

$$\frac{\delta_e^*}{D^*} = \frac{2.4}{(C_H Re_D)^{1/2}}\left[1 + 0.11\,Tu_\infty Re_D\frac{\lambda_\infty^*}{D^*}\right]^{1/2} \qquad (11)$$

The parameter C_H has a value of 4.0 from potential flow theory. In practice C_H is approximately 3.7, Kwon, et al. (1983) for flows at high Re_D and low freestream turbulence in facilities with negligible tunnel blockage. In general, C_H is a function of Tu_∞, the flow blockage parameter, and Re_D. These effects are implicitly included in equation (11) by the terms between the brackets, thus C_H is taken as 3.7 in our analysis.

Outside the near-wall viscous region, the mean velocity is given by

$$\overline{V}_e^* = -c^* y^* \qquad (12)$$

At the edge of the near-wall viscous region, y^* is equal to δ_e^*, leading to

$$\frac{\overline{V}_e^*}{\overline{V}_\infty^*} = \frac{\beta_{02}}{Re_D^{1/2}} \qquad (13)$$

$$\beta_{02} = 2.4C_H^{1/2}\left[1 + 0.11\,Tu_\infty Re_D\frac{\lambda_\infty^*}{D^*}\right]^{1/2} \qquad (14)$$

When the freestream Reynolds number is large relative to unity, $|X_p^{*'}|$ from equation (8) and evaluated at $y^* = \delta_e^*$ becomes

$$|X_p^{*'}|_e = \frac{\lambda_e^*}{2\pi}\left|\frac{U_e^{*'}}{U_\infty^{*'}}\right| Iu_\infty Re_D^{1/2}\left[b_{02} + Iv_\infty Re_D^{1/2}\frac{V_e^{*'}}{|V_\infty^{*'}|}\right]^{-1} \qquad (15)$$

At the edge of the near-wall viscous region, $|X_p^{*'}|_e$ is equivalent to the magnitude of an oscillation in the velocity profile. These oscillations are included in the assumed edge velocity by the parameters b_n^*. Therefore, setting b_n^* equal to $|X_p^{*'}|_e$ and defining e_n as the normalized fluctuating energy for mode n yields

$$b_n^* = \frac{e_n}{2\pi}\lambda_e^*\left|\frac{U_e^{*\prime}}{U_\infty^{*\prime}}\right| Iu_\infty Re_D^{1/2}\left[\beta_{02} + Iv_\infty Re_D^{1/2}\frac{V_e^{*\prime}}{\left|V_\infty^{*\prime}\right|}\right]^{-1} \qquad (16)$$

Equatinn (16) provides a description for the oscillation parameters based upon the simplified vortex model. However, λ_e^*, Iu_∞, and Iv_∞ are generally not measured in experimental studies. Two assumptions will be useful here. The first assumes the freestream turbulence is approximately isotropic. The second assumes λ_e^* is equal to λ_∞^*. Thus, equation (16) written in nondimensional form becomes

$$\beta_n = \beta_{01} e_n\left(\frac{\lambda_\infty^*}{D^*}\right)\left|\frac{U_e^{*\prime}}{U_\infty^{*\prime}}\right|\frac{Tu_\infty Re_D^{1/2}\left|\frac{V_e^{*\prime}}{V_\infty^{*\prime}}\right|}{\beta_{02} + Tu_\infty Re_D^{1/2}\left|\frac{V_e^{*\prime}}{V_\infty^{*\prime}}\right|} \qquad (17)$$

where $\beta_{01} = 90/\pi$. The constant β_{01} arises from nondimensionalizing b_n^* by the scale $b^* = D^*/180$.

Pulsation Parameters, a_n

As the oscillation parameters are related to the fluctuations in the x^* direction, the pulsation parameters are related to the fluctuations in the y^* direction. Therefore, each individual fluctuation, a_n, is given by

$$a_n = e_n\frac{\left|V_e^{*\prime}\right|}{\overline{V}_e^*} \qquad (18)$$

writing a_n as

$$a_n = e_n\frac{\left|V_e^{*\prime}\right|}{\left|V_\infty^{*\prime}\right|}\frac{\left|V_\infty^{*\prime}\right|}{\overline{V}_\infty^*}\frac{\overline{V}_\infty^*}{\overline{V}_e^*}$$

and using equation (13) yields

$$a_n = e_n\frac{Tu_\infty Re_D^{1/2}}{\beta_{02}}\frac{\left|V_e^{*\prime}\right|}{\left|V_\infty^{*\prime}\right|} \qquad (19)$$

This final expression also assumes isotropic turbulence in the freestream. The parameter e_n again represents the percentage of the fluctuating energy in mode n compared with the total fluctuating energy.

Energy Parameters, e_n

The parameter e_n, introduced above, represents the amount of energy in mode n compared with the total energy in fluctuating modes. Theoretically, the summation of the e_n across the energy spectrum should be one. Therefore, e_n is a nondimensional fluctuating energy. It is the fluctuating energy at mode n divided by the total fluctuating energy.

To simplify the task of quantifying the nondimensinnal fluctuating energy parameters, several assumptions are useful:

(i) The turbulence in the freestream is at least approximately isotropic.

(ii) The freestream turbulence modes at the highest wave numbers are dissipated before reaching the edge of the near-wall viscous region.

For an isotropic flnw, Hinze (1975, p. 205) gives the turbulence intensity as a function of the three-dimensional energy-spectrum function, $E^*(\kappa^*,t^*)$.

$$\frac{3}{2}Tu^2\overline{V}^{*2} = \int_0^\infty E^*\left(\kappa^*,t^*\right)d\kappa^*$$

$$\kappa^* = \frac{n\Omega^*}{\overline{V}^*} \qquad (20)$$

Here κ^* is the dimensional wave number, t^* is the dimensional time, n is the nondimensional frequency, and Ω^* is the characteristic frequency of the freestream unsteadiness. Nondimensionally, the variables above are

$$E(\kappa,t) = \frac{\hat{\kappa}^* E^*\left(\kappa^*,t^*\right)}{\overline{V}^{*2}} \qquad \kappa = \frac{\kappa^*}{\hat{\kappa}^*}$$

$$\frac{3}{2}Tu^2 = \int_0^\infty E(\kappa,t)\,d\kappa \qquad (21)$$

The parameter $\hat{\kappa}^*$, which is at the center of the range of energy-containing eddies, is the wave number at which $E^*(\kappa^*,t^*)$ is a maximum.

Again for an isotropic flow, Hinze (1975, p. 247) presents the von Karman interpolation function for $E^*(\kappa^*,t^*)$. The von Karman function is fairly accurate at the lower wave numbers, including the range of the energy-containing eddies, but it deviates at the highest wave numbers.

$$E^*\left(\kappa^*,t^*\right) = \frac{55}{9}\frac{\Gamma(5/6)}{\sqrt{\pi}\,\Gamma(1/3)}\frac{Tu^2\overline{V}^{*2}}{\hat{\kappa}^*}\frac{\left(\frac{\kappa^*}{\hat{\kappa}^*}\right)^4}{\left[1+\left(\frac{\kappa^*}{\hat{\kappa}^*}\right)^2\right]^{17/6}}$$

$$E(\kappa,t) = 1.4528\,Tu^2\frac{\kappa^4}{\left[1+\kappa^2\right]^{17/6}} \qquad (22)$$

The gamma function is denoted by Γ. An analysis of equation (22) reveals that $E(\kappa,t)$ is a maximum when κ is $2\sqrt{3/5} = 1.5492$ rather than unity as the definitions above would imply. So that $\hat{\kappa}$ will correspond to the peak value of $E(\kappa,t)$, a value of 1.5492 will be used for $\hat{\kappa}$ in the work which follows.

From the introduction above, the definition for e_n comes in two parts. From equations (19) and (21), and the relation between a_n and the edge turbulence intensity presented below, e_n^2 is proportional to $E(\kappa_n,t)$. More specifically,

$$e_n \propto \frac{a_n}{Tu} \propto \frac{\sqrt{E(\kappa_n,t)}}{Tu}$$

Further, as a result of assumption (ii), the individual values of e_n^2 must, over the entire energy spectrum, sum to unity.

$$e_{nn}^2 \equiv \frac{2}{3}\frac{E(\kappa_n,t)}{Tu^2} = 0.96850\frac{\kappa_n^4}{\left[1+\kappa_n^2\right]^{17/6}} \qquad (23)$$

$$e_n^2 \equiv \frac{e_{nn}^2}{\sum_i^N e_{ni}^2} \qquad (24)$$

The normalization presented by the first equality in equation (23) is suggested by the integration of the three-dimensional energy spectrum function given by equation (21). Discretizing e_n^2 as indicated by equation (23) is equivalent to a numerical integration of the energy spectrum using the midpoint rule.

Because the e_n are effectively part of a numerical integration of a peaked function, $E(\kappa,t)$, an odd number of components is selected. Further, the nondimensional frequency of the component in the middle of the distribution, $\hat{n}$, will correspond to the wave number $\hat{\kappa}$. Therefore, an appropriate form for the wave number κ_n for use with equation (23) may be defined.

$$\kappa_n = \hat{\kappa}\frac{n}{\hat{n}} \qquad (25)$$

For only one component in the series (N=1) e_1 is unity. For a series of five components (N=5) the middle component is the third, so $\hat{n}$ is 3, and the values for e_n are tabulated below.

Table 1: Values of e_n for an Edge Parameter Series of Five Components

$n/\hat{n}$	κ_n	e_{on}^2	e_n^2	e_n
1/3	0.51640	0.035250	0.05478	0.23405
2/3	1.0328	0.14089	0.21894	0.46791
1	1.5492	0.17405	0.27047	0.52007
4/3	2.0656	0.15919	0.24738	0.49737
5/3	2.5820	0.13413	0.20843	0.45654
Sum		0.64351	1.00000	2.17594

Distortion Effects Due to Mean Strain

The expressions for the pulsation and oscillation parameters included terms which account for the amplification and attenuation of the fluctuating components by the mean strain field as the unsteady flow approaches the stagnation region. To account for this effect, rapid distortion theory is used.

Rapid distortion theory describes the deformation of turbulence solely due to an external strain field. For turbulence convected by a flow approaching a two-dimensional stagnation point, the mean flow creates the strain field. If the turbulence is not also deformed by nonlinear interactions while it is swept by the body, such as viscous dissipation, then the turbulence experiences a rapid distortion due to passing the body. Hunt (1973) developed theoretical expressions for the local stresses about a blunt body in crossflow due to a rapid distortion.

- The approaching fluid is assumed to be incompressible.
- For large eddies, when $\lambda_\infty^*/D^* \to \infty$, $V^{*'}$ decreases, $U^{*'}$ increases and $W^{*'}$ does not change. The relevant results along the mean stagnation streamline for the present model are

$$\frac{\overline{V_e^{*'}V_e^{*'}}}{V_\infty^{*'}V_\infty^{*'}} \equiv 2 - \frac{\bar{V}_e^*}{\bar{V}_\infty^*}$$

- For eddies which are roughly the same size as the cylinder diameter, when λ is unity, the turbulence components generally were not amplified nor attenuated from their freestream values.
- For small eddies, when $\lambda_\infty^*/D \to 0$, $V^{*'}$ increases, $U^{*'}$ decreases and $W^{*'}$ increases (by less than $V^{*'}$). These results, originally developed by Batchelor and Proudman (1954) on the mean stagnation streamline are

$$\frac{\overline{U_e^{*'}U_e^{*'}}}{V_\infty^{*'}V_\infty^{*'}} \approx \frac{3}{4}\frac{\bar{V}_e^*}{\bar{V}_\infty^*}\left[\ln\left(\frac{4\bar{V}_\infty^*}{\bar{V}_e^*}\right)-1\right]$$

$$\frac{\overline{V_e^{*'}V_e^{*'}}}{V_\infty^{*'}V_\infty^{*'}} \equiv \frac{3}{4}\left[\frac{\bar{V}_\infty^*}{\bar{V}_e^*}+\frac{1}{2}\frac{\bar{V}_e^*}{\bar{V}_\infty^*}\ln\left(\frac{4\bar{V}_\infty^*}{\bar{V}_e^*}\right)\cdots\right]$$

Using the expression for $\bar{V}_e^*$ from equation (13), we can summarize the results below when λ_∞^*/D^* is much greater than unity:

$$\frac{\overline{V_e^{*'}V_e^{*'}}}{V_\infty^{*'}V_\infty^{*'}} \equiv \frac{\beta_{02}}{Re_D^{1/2}} \qquad \frac{\overline{V_e^{*'}V_e^{*'}}}{V_\infty^{*'}V_\infty^{*'}} \equiv \frac{\beta_{02}}{Re_D^{1/2}} \qquad (26a,b)$$

$$\lambda_\infty^*/D^*\frac{\overline{U_e^{*'}U_e^{*'}}}{V_\infty^{*'}V_\infty^{*'}} \equiv \frac{3}{4}\frac{\beta_{02}}{Re_D^{1/2}}\left[\ln\left(4\frac{Re_D^{1/2}}{\beta_{02}}\right)-1\right] \qquad (27\,a)$$

$$\frac{\overline{V_e^{*\prime} V_e^{*\prime}}}{\overline{V_\infty^{*\prime} V_\infty^{*\prime}}} \equiv \frac{3}{4}\left[\frac{Re_D^{1/2}}{\beta_{02}} + \frac{1}{2}\frac{\beta_{02}}{Re_D^{1/2}} \ln\left(4\frac{Re_D^{1/2}}{\beta_{02}}\right)\right] \quad (27\,b)$$

While equations (26) and (27) are accurate for the limiting values of λ_∞^* / D^*, most real cases, including experiments, fall somewhere between these extremes. As a first approximation at expressions for any λ_∞^* / D^*, an exponential combination of the expressions in (26) and (27) is suggested by the data taken by Britter, Hunt, and Mumford (1979). The basic form of the proposed interpolating function is

$$Z_j = \zeta_{ja}\left[1 + \zeta_{jb} exp\left(\zeta_{jc}\lambda\right)\right] \quad (28)$$

In this form λ is the nondimensional integral length scale, λ_∞^* / D^*, Z_j is the normalized fluctuation correlation, and ζ_{ja}, ζ_{jb}, and ζ_{jc} are constants. The subscript 'j' may be either U or V.

$$Z_V = \left|\frac{v_e^{*\prime}}{v_\infty^{*\prime}}\right|^2 = \frac{\overline{v_e^{*\prime} v_e^{*\prime}}}{V_\infty^{*\prime} V_\infty^{*\prime}} \qquad Z_V = \left|\frac{v_e^{*\prime}}{v_\infty^{*\prime}}\right|^2 = \frac{\overline{v_e^{*\prime} v_e^{*\prime}}}{V_\infty^{*\prime} V_\infty^{*\prime}} \quad (29)$$

Three known values of Z_j are necessary to determine the constants in the general form (28). From the rapid distortion expressions above, Z_j is known as λ approaches zero and as λ approaches infinity. The final constant is set from experimental data using the point where Z_j is unity, λ_{1j}. From the data presented in Britter, Hunt, and Mumford (1979), λ_{1V} is approximately 1.12. Because the lateral integral length scale is roughly half of the longitudinal integral length scale within a grid-generated turbulent flow, Hinze (1975) λ_{1U} should be one half of λ_{1V}.

$$Z_j = Z_{\infty j} + \left(Z_{0j} - Z_{\infty j}\right) exp\left[\frac{\lambda}{\lambda_{1j}} ln\left(\frac{Z_{1j} - Z_{\infty j}}{Z_{0j} - Z_{\infty j}}\right)\right] \quad (30)$$

The constant $Z_{\infty j}$ refers to the expressions from equation set (26), Z_{0j} refers to equation set (27), and Z_{1j}, which here is unity, refers to the values at λ_{1j}.

Nondimensional Fraquency, α_Ω

The nondimensional frequency, α_Ω, which appears in equation (4) is defined as

$$\alpha_\Omega^2 \equiv \frac{\Omega^*}{c^*} = \frac{D^* \Omega^*}{c_{H1} \overline{V}_\infty^*} \quad (31)$$

The frequency of the large-scale unsteadiness may be expressed in terms of the local freestream velocity and the longitudinal integral length scale, λ^*.

$$\Omega^* = 2\pi \frac{\overline{V}^*}{\lambda^*} \quad (32)$$

The magnitude of the mean velocity at the edge of the boundary layer is

$$\overline{V}_e^* = \beta_{02} \overline{V}_\infty^* Re_D^{-1/2} \quad (33)$$

Thus at the edge of the boundary layer where y^* is δ_e^*

$$\alpha_\Omega^2 = 2\pi \frac{D^*}{\lambda_e^*} \frac{\beta_{02}}{C_H Re_D^{1/2}} \quad (34)$$

Assuming $\lambda_e^* / \lambda_\infty^*$ is equal to 1 yields

$$\alpha_\Omega^2 = 7.84 \frac{D^*}{\lambda_\infty^*}\left[1 + 0.11\, Tu_\infty Re_D \frac{D^*}{\lambda_\infty^*}\right]^{1/2} Re_D^{-1/2} \quad (35)$$

Physical Interpretation of the Model

The model presented in this paper represents a first approximation for a very complex flow field. It does, however, contain what are thought to be the essential parameters necessary to describe the effect of a turbulent freestream upon the stagnation-point heat transfer rate. These parameters are the freestream turbulence intensity, Tu_∞, the longitudinal integral length scale, λ_∞, and the Reynolds number, Re_D. These parameters appear naturally as part of the derivation. In this sense this analysis represents a more fundamental approach in that experimental correlations or curve fits were not employed. This model does contain several important assumptions and approximations which are:

- The vorticity model assumes that the freestream turbulence is generated by a turbulent wake, or free shear layer, which is characterized by large coherent structures.
- The vortical structures are assumed to be quasi-two-dimensional with their vorticity aligned with the body's spanwise axis.
- The large-scale, coherent structures are assumed to exist only at a few discrete frequencies or length scales.
- The effect of these coherent structures modifies the edge velocity and mean pressure gradient through the pulsation parameter, a_n, the oscillation parameter, β_n, and the frequency parameter, α_Ω.
- The analysis ignores the existence of small-scale, random turbulence that may be entrained within the stagnation region boundary layer.

A sketch of the near-wall viscous region, Figure 4, shows a typical coherent structure about to impinge upon the edge of the boundary layer denoted by δ_e^* which is defined in equation (11). For typical freestream parameters found in a gas turbine, δ_e^*/D^* varies between 0.005 and 0.05. The width of the stagnation region is characterized by the oscillation parameter, b_n^*. In the analysis, the coordinate x^* and the oscillation parameter are scaled by $b^* = D^*/180$. From equations (16) and (17), $\beta_n = b_n^*/b^*$ and is nearly independent of Re_D. Calculations confirm that β_n varies by less than 10 percent when Re_D varies from 5×10^4 to 10^6. However, β_n varies almost linearly with λ. In most of the

numerical simulations, $\beta_n \le 1$. Its maximum value is approximately 10 when $Tu_\infty Re_D^{1/2} = 60$ and $\lambda = 0.5$. These values correspond to an oscillation of roughly ±10 degrees about the mean stagnation point or a displacement of ±0.056 D^*. Thus, with this scaling, the edge of the unsteady boundary layer and the width of the oscillation are approximately the same.

The pulsation parameter, a_n, has a more complex behavior which is seen by writing equation (19) as

$$a_n = e_n \frac{Tu_\infty Re_D^{1/2}}{2.4\, C_H \left[1 + 0.1\, Tu_\infty Re_D \frac{\lambda_\infty^*}{D^*}\right]^{1/2}} \left|\frac{U_e^{*'}}{V_\infty^{*'}}\right| \qquad (37)$$

For large values of $Tu_\infty Re_D$, a_n varies inversely with λ. In most of the numerical solutions, a_n varies from approximately 2 to 5.

An important characteristic to note in this unsteady edge model is that the unsteady velocities in the stagnation region are large compared to the mean velocities. In fact, for most values typical of freestream turbulence, $\left|V_e^{*'}\right| / \left|\overline{V}_e^*\right|$, which is equal to a_n, and $\left|U_e^{*'}\right| / \left|\overline{U}_e^*\right|$, which is proportional to β_n, are greater than unity at $x = 0$. Thus, the stagnation region boundary layer is highly unsteady.

A final point concerning the pulsation parameter can be made by evaluating a_n at $y_e = 1$, and noting that $y = y^*\left(c^*/\nu_\infty^*\right)^{1/2}$ and $V_e = V_e^* / \left(c^* \nu_\infty^*\right)^{1/2}$. For this case, a_n becomes

$$a_n\big|_{y_e=1} = e_n \frac{\left|V_e^{*'}\right|}{\left(c^* \nu_\infty^*\right)^{1/2}} = e_n \frac{\left|V_\infty^{*'}\right|}{\left(c^* \nu_\infty^*\right)^{1/2}} \left|\frac{V_e^{*'}}{V_\infty^{*'}}\right| \qquad (38)$$

In terms of the turbulence parameter, Tu_a, defined by Dullenkopf and Mayle (1995), this expression becomes

$$a_n = e_n Tu_a \left|\frac{V_e^{*'}}{V_\infty^{*'}}\right|$$

The effective turbulence level, Tu_{eff}, is obtained by integrating over the energy spectrum, or in our case by summing over the discretized spectrum. Thus Tu_{eff} defined in this manner is analogous to their $Tu\lambda$ apart from the turbulence attenuation factor $\left|V_e^{*'}\right| / \left|V_\infty^{*'}\right|$.

The final model parameter is the nondimensional frequency, α_Ω. It enters the model through the pressure gradient defined in equation (4). It also appears in the nondimensional form of the boundary layer equations as an important scaling parameter. Physically the nondimensional frequency measures the unsteadiness and relates the unsteady diffusion of momentum (vorticity) inside the boundary layer to the mean momentum. From equation (31) and Figure 4, we see that $\alpha_\Omega^2 \propto \delta_H^* / \delta_s^*$.

In conclusion, a model for the effect of a specific type of freestream turbulence is presented. It contains three nondimensional parameters. By inspecting the forms for these parameters, all three parameters are functions of Tu_∞, Re_D, and λ_∞^* / D^*.

RESULTS AND DISCUSSION

There are two levels at which the unsteady velocity model can and should be validated by comparing to experimental data. Obviously, from the perspective of an engineering analysis and design tool the model must be able to predict the surface heat transfer for given freestream turbulent parameters. But also, on a more fundamental level, the unsteady fluctuations which the turbulent freestream imposes upon the edge of the boundary layer should be accurately represented. To validate the model at this level is difficult because most researchers do not report the necessary components of the turbulence intensity needed to check a model. Further, if this information is given the sampling location is often outside of the boundary layer for a stagnation point flow due to instrumentation limitations. Nevertheless, an attempt is presented here to quantify the model in some approximate sense at this fundamental level.

Validation of the Model Parameters, a_n and β_n

Hijikata, Yoshida, and Mori (1982) provide measurements for the amplification of the turbulence intensity as the flow approaches the stagnation region of a two-dimensional cylinder. Specifically, they measured the radial and circumferential components of turbulence intensity along the mean stagnation streamline from an upstream position where the turbulence was effectively isotropic to positions close to the cylinder surface. At a position near the cylinder but outside the boundary layer the pertinent values are:

$Re_D = 54{,}000$ $\qquad$ $\lambda_\infty^* / D^* = 0.09$

$Tu = 0.052$ $\qquad$ $Tu_{e,y} = 0.42$ $\qquad$ $Tu_{e,x} = 0.30$

The pulsation parameter, a_n, in this model equals the magnitude of the fluctuating velocity divided by the average velocity normal to the stagnation point at the edge of the boundary layer. For a single component, $N = 1$, the value for a_1 is given by

$$a_1 = e_1 \frac{\left|V_e^{*'}\right|}{\overline{V}_e^*} = e_1 \frac{Tu_\infty Re_D^{1/2}}{\beta_{02}} \left|\frac{V_e^{*'}}{V_\infty^{*'}}\right|$$

Using the experimental values for Tu_∞ and Re_D and equations (14) and (27 b) we find $a_1 = 0.453$. This agreement is within 7 percent of the experimental value for $Tu_{e,y}$. While this agreement is excellent, it should be noted that the experimentally determined $Tu_{e,y}$ was taken at $y^*/D^* = 0.1$ while the corresponding theoretical value from equation (11) is $\delta_e^*/D^* = 0.03$.

The next task is finding $\left|U_e^{*''}\right| / \overline{V}_e^*$. Setting N = 1 and extracting the fluctuating component from U_e in equation (3 a) gives $\left|U_e^{*''}\right| = \beta_1 \left(c^* b^*\right)$. Finally, dividing by $\overline{V}_e^*$ yields

$$\frac{\left|U_e^{*''}\right|}{\overline{V}_e^*} = \frac{C_H}{180} \frac{Re_D^{1/2}}{\beta_{02}} \beta_1 \tag{36}$$

From equation (17) $\beta_1 = 0.71$, thus $\left|U_e^{*''}\right| / \overline{V}_e^* = 0.14$ while the corresponding experimental value is $Tu_{e,\theta} = 0.30$. Here the cause for the poor agreement is directly related to the strong attenuation of the turbulent fluctuations very near the body's surface. Equation (27 a) gives $\left|U_e^{*''}\right| / \overline{V}_\infty^{*''} = 0.085$. Upon adjusting the location to $\delta_e^*/D^* = 0.1$. to be consistent with the experiment, we find that $\left|U_e^{*''}\right| / \overline{V}_e^* = 0.32$. Although this test cannot be considered as a validation of the model, it does provide some level of confidence.

Heat Transfer Predictions

The ultimate test for any theoretical model is its ability to predict quantities of engineering interest with acceptable accuracy. The key word here is "predict", since many semi-empirical models can reproduce experimentally measured quantities by proper adjustment of the model parameters. The quantity of engineering interest is surface heat transfer or its nondimensional representation given by the Nusselt number.

The local Nusselt number based on the cylinder diameter, D^*, the dimensional surface heat flux, $q_w^{*''}$, and the thermal conductivity of the fluid, k^*, is

$$Nu_D \equiv \frac{q_w^{*''} D^*}{k^* \left(T_w^* - T_\infty^*\right)} = - \frac{D^*}{\left(T_w^* - T_\infty^*\right)} \left(\frac{\partial T^*}{\partial y^*}\right)_{y^*=0}$$

The unsteady response within the near-wall viscous region, or boundary layer, can be determined by solving the instantaneous momentum and energy equations. This solution approach analytically decomposes the nondimensional governing equations into time-independent and time-dependent expressions. The time-dependence is modeled with a few frequencies and is defined using a finite Fourier expansion in time. The individual time-dependent expressions are further simplified for the current application by using a high-frequency approximation. This model has been used successfully in both incompressible and compressible formulations.

Details of the formulation and solution of the mean (time-averaged) and unsteady boundary layer equations for an incompressible flow are given by Hanford and Wilson (1994). Interested readers should consult this reference for the details. The corresponding compressible formulation can be found in the dissertation by Hanford (1994). The incompressible code was used to predict the temperature gradient from which the Nusselt number was determined. No arbitrary parameters were adjusted in an attempt to match the experimental data. Results of the model predictions are given in Figures 5 and 6. The general trends and qualitative features of the model are discussed below and contrasted with the experimental data in Figures 1 and 2.

The review of the literature revealed a wide range of experimental results as shown in Figures 1 and 2. This variation arises because the correlating groups $Nu_D / Re_D^{1/2}$ and $Tu_\infty Re_D^{1/2}$, are not completely adequate to describe the existing data. Most researchers claim that heat transfer always increases with Reynolds number, while others maintain that Reynolds number has little effect on surface heat transfer. The data in Figure 1 does show a general trend with Reynolds number. The largest values of heat transfer occurred for the highest Reynolds number experiments and the lowest values occurred for the very low Reynolds number tests. The numerical predictions, as presented in Figure 5, suggest that heat transfer increases as Reynolds number increases when the nondimensional scale of turbulence is constant. The value of λ in Figure 5 was taken as 0.032.

For all but the largest Reynolds number studied the predicted heat transfer augmentation per unit increase in turbulence intensity increases as the magnitude of the turbulence intensity increases, reaches a maximum, and then slowly decreases. This apparent saturation of the heat transfer augmentation at large turbulence intensities shown in Figure 5 is confirmed in the experimental studies. Physically, saturation of the heat transfer represents the laminar region near the wall becoming fully disrupted by the unsteadiness convected from the outer flow. This effect is accounted for in the model because the pulsation and oscillation parameter depend upon location of the near-wall viscous region, δ_e^x. Since δ_e^x increases with $Tu_\infty^{1/2}$, both a_n and β_n asymptotically approach a limiting value. At a Reynolds number of 10^6 however, the predicted surface heat-transfer augmentation did not saturate at larger values of turbulence intensity. The reason for this behavior is not clear and may represent a shortcoming in the current model. Since, the largest values of Reynolds number in the experimental data sets was 302,000 it would be premature to draw any definite conclusions.

The work of Yardi and Sukhatme (1978) predict a maximum in the stagnation-point heat transfer when the parameter $\lambda Re_D^{1/2}$ is roughly 10. Their experiments used Reynolds numbers from 6000 up to 100,000, nondimensional turbulence scales from 0.03 up to 0.38, and $Tu_\infty Re_D^{1/2}$ up to 20. For these values $\lambda Re_D^{1/2} = 10$. For Re_D = 100,000, we find that λ = 0.032. The numerical predictions for $Nu_D / Re_D^{1/2}$ as a function of λ are illustrated in Figure 6 for a Reynolds number of 100,000. For the range of nondimensional length scales investigated, the maximum heat transfer in Figure 6 occurs when λ = 0.1. Although, this length scale is off by a factor of three compared to the experimental result, the model does confirm Yardi and Sukhatme's findings in a qualitative sense. Specifically, the model predicts that the heat transfer increases with λ, reaches a maximum value for moderate λ, then decreases as λ continues to increase. Recall that β_n increases almost linearly with λ. Large values of β_n imply large excursions of the stagnation point from it mean position. Thus, the mean heat transfer rate is expected to decrease. Additionally, a_n decreases when λ increases so that the effect is even more pronounced.

On the basis of these preliminary predictions, the model seems to have captured some of the physical mechanisms of turbulent augmented heat transfer. Its strength is that it represents the appropriate physics of the flow to a first approximation, and it does produce experimentally observed trends.

There were several approximations made in the model during the initial formulation which could be improved. Perhaps the most important one concerns the assumption that $\lambda_-^* = \lambda_e^*$. We attempted to improve this approximation by approximating the effect of the inviscid strain field on turbulent length scale. However, the complications associated with this approach appeared to outweigh the advantage. A second source of potential error in the numerical predictions is associated with the number of individual frequencies included in the unsteady edge model. At most, we have included five discrete frequencies. In the compressible calculations we have been limited to only one due to computational limitations. An alternate numerical scheme for the boundary layer solver would remedy this limitation and this is being considered.

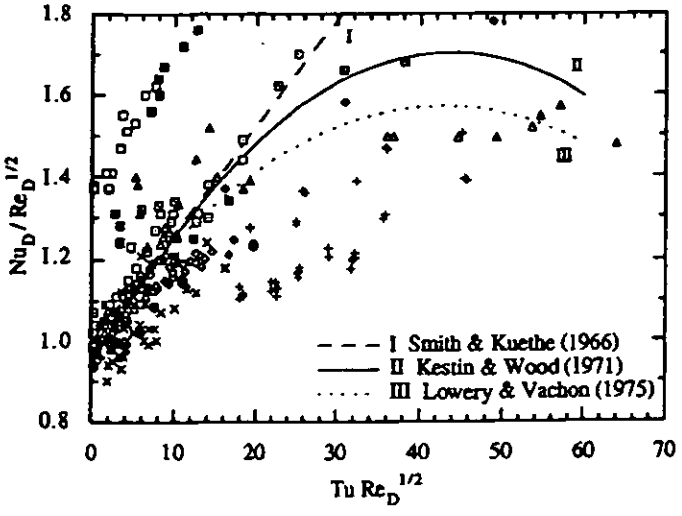

Figure 1:
The augmented stagnation-point heat-transfer measurements displayed. The individual data are taken from: ⊠, Zapp (1950), ■, Giedt (1951), ▲, Seban (1960), ⊞, Kestin, Maeder, and Sogin (1961), □, Appelqvist (1965), ⊡, Smith and Kuethe (1966), ◇, Kayalar (1969), ◆, Dyban, Epick, and Kozlova (1974), ●, Sikmanovic, Oka, and Koncar-Djurdjevic (1974), △, Lowery and Vachon (1975), ×, Yardi and Sukhatme (1978), and +, Ames and Moffat (1990). The correlation curves are taken from: I, Smith and Kuethe (1966), II, Kestin and Wood (1971), and III, Lowery and Vachon (1975).

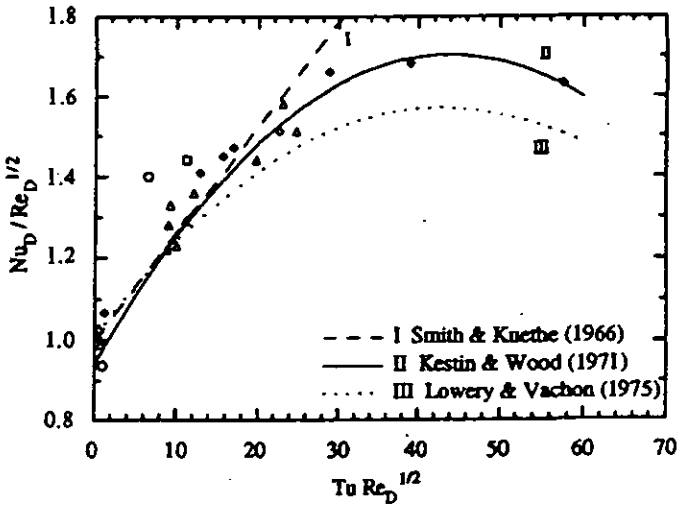

Figure 2
The augmented stagnation-point mass-transfer measurements converted to equivalent heat transfer data and displayed. The individual data are taken from: □, Sogin and Subramanian (1961), ○, Brun, Diep, and Kestin (1966), △, Kestin and Wood (1971), and ◇, Van Dresar and Mayle (1988). The curves are taken from: I, Smith and Kuethe (1966), II, Kestin and Wood (1971), and III, Lowery and Vachon (1975).

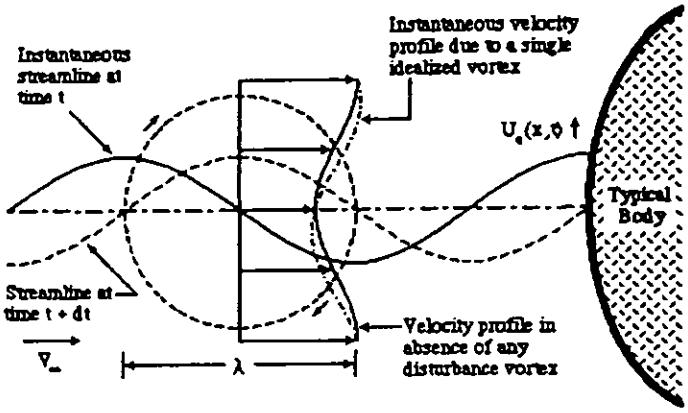

Figure 3.
Simplified vorticity model: Stagnation point fluctuation due to a single wavelength vortical structure convected by the mean flow.

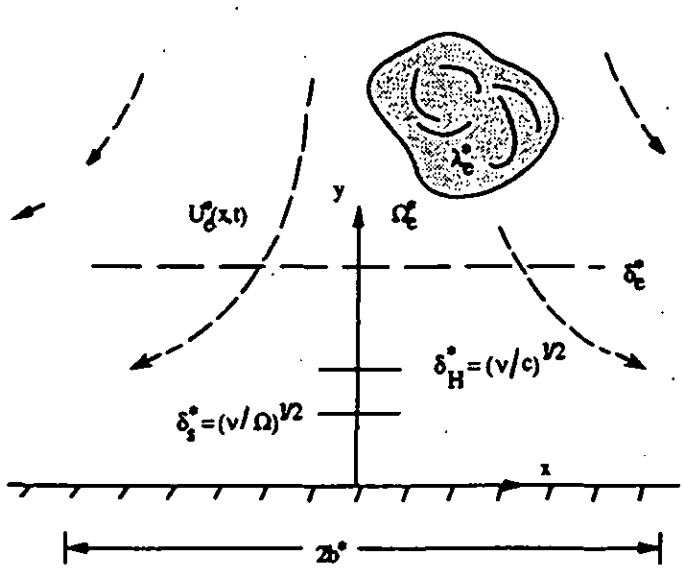

Figure 4:
Sketch of the near-wall viscous region showing a turbulent structure about to impinge on the boundary layer.

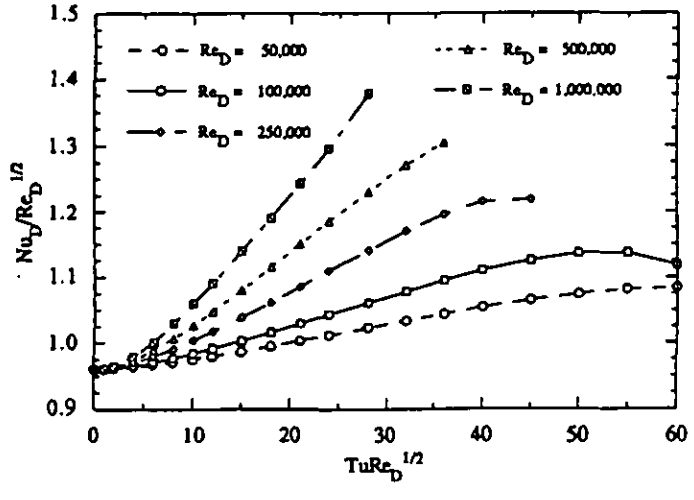

Figure 5:
Nondimensional heat transfer vs. $Tu\,Re_D^{1/2}$ for $\lambda^*_\infty / D^* = 0.032$.

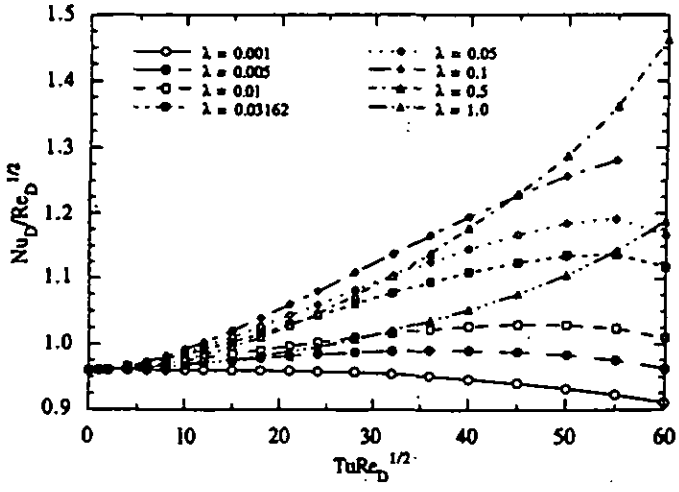

Figure 6:
Nondimensional heat transfer vs. $Tu\,Re_D^{1/2}$ for $Re_D = 10^5$.

ACKNOWLEDGMENT

This work has been supported by NASA Langley Research Center through grant NAG 1.1364. Support was also received from the Institute for Advanced Technology at the University of Texas at Austin.

REFERENCES

AMES, F.E., and MOFFAT, R.J. (1990) "Heat Transfer with High Intensity, Large Scale Turbulence: The Flat Plate Turbulent Boundary Layer and the Cylindrical Stagnation Point", Report HMT-44, Department of Mechanical Engineering, Stanford University, Stanford, California.

APPELQVIST, J.D., II (1965) "The Influence of Turbulence on the Local Heat Transfer from a Cylinder Normal to an Air Stream, Including Further Development of a Method for Local Heat Transfer Measurements", Doctoral Dissertation, Institute of Applied Thermo and Fluid Dynamics, Chalmers University of Technology, Gothenburg, Sweden.

BOGUCZ, E.A., DIRIK, E.A., and LYMAN, F.A. (1988) "Unsteady Stagnation-Point Heat Transfer due to the Motion of Freestream Vortices," *AIAA/ASME/SIAM/APS First National Fluid Dynamics Congress, 3*, AIAA, Washington, D.C., pp. 1893-1900.

BRITTER, R.E., HUNT, J.C.R., and MUMFORD, J.C. (1979) "The Distortion of Turbulence by a Circular Cylinder", *Journal of Fluid Mechanics, 92*, pp. 269-301.

BRUN, E.A., DIEP, and KESTIN, J. (1966) "Sur un nouveau type des tourbillons longitudinaux dans l'ecoulement autour d'un cylindre. Influence de l'angle d'attaqiu et de la turbulence du courant libre", *Comptes Rendus de l'Academie des Sciences Paris, Series A, 263*, pp. 742-745. [In French]

CEBECI, T., KRAINER, A., SIMONEAU, R.J., and PLATZER, M.F. (1987) "A General Method for Unsteady Stagnation Region Heat Transfer and Results for Model Turbine Flows", *Proceedings of the 1987 ASME-JSME Thermal Engineering Joint Conference, Honolulu, Hawaii, 2*, ASME, New York, New York, pp. 541-646.

DRIVER, D.M., SEEGMILLER, H.L., and MARVIN, J.G. (1987) "Time-Dependent Behavior of a Reattaching Shear Layer", AIAA Journal, 25, pp. 914-919.

DULLENKOPF, K. and MAYLE, R. E. (1994) "The Effects of Incident Turbulence and Moving Wakes on Laminar Heat Transfer in Gas Turbines", *Journal of Turbomachinery, 116*, pp. 23-28.

DULLENKOPF, K. and MAYLE, R. E. (1995) "An Account of Free-Stream-Turbulence Length Scale on Laminar Heat Transfer", *Journal of Turbomachinery, 117*, pp. 401-406.

DYBAN, E.P., EPICK, E.YA., and KOZLOVA, L.G. (1974) "Combined Influence of Turbulence Intensity and Longitudinal Scale and Air Flow Acceleration on Heat Transfer of Circular Cylinder", FC8.4, *Heat Transfer 1974: Proceedings of the Fifth International Heat Transfer Conference, Tokyo, Japan 1974, 2*, Hemisphere Publishing Corporation, Washington, D.C., pp. 310-314.

GIEDT, W.H. (1951) "Effect of Turbulence Level of Incident Air Stream on Local Heat Transfer and Skin Friction on a Cylinder", *Journal of the Aeronautical Sciences, 18*, pp. 725-730, 766.

HANFORD, A.J. (1994) "The Augmentation of Stagnation Point Heat Transfer by Quasi-Periodic Freestream Fluctuations", Doctoral Dissertation, The University of Texas at Austin, Austin, Texas.

HANFORD, A.J., and WILSON, D.E. (1994) "The Effect of a Turbulent Wake on the Stagnation Point: Part II - Heat Transfer Results", *Journal of Turbomachinery*, **116**, pp. 46-54. Also: ASME Paper 92-GT-197.

HIJIKATA, K., YOSHIDA, H. and MORI, Y. (1982) "Theoretical and Experimental Study of Turbulence Effects on Heat Transfer Around the Stagnation Point of a Cylinder", FC30, *Heat Transfer for 1982, Proceedings of the Seventh International Heat Transfer Conference, Munich, West Germany 1982, 3*, Hemisphere Publishing Corporation, Washington, D.C., pp. 165-170.

HINZE, J.O. (1975) *Turbulence*, Second Edition, McGraw-Hill Book Company, Incorporated, New York, New York.

HOSHIZAKI, H., CHOU, Y.S., KULGEIN, N.G., and MEYER, J.W. (1975) "Critical Review of Stagnation Point Heat Transfer Theory", Technical Report AFFDL-TR-75-85, Wright-Patterson Air Force Base, Dayton, Ohio, pp. 1-100.

HUNT, J.C.R. (1973) "A Theory of Turbulent Flow Round Two-Dimensional Bluff Bodies", *Journal of Fluid Mechanics, 61*, pp. 625-706.

ISHIGAKI, H. (1970) "Periodic Boundary Layer Near a Two-Dimensional Stagnation Point", *Journal of Fluid Mechanics, 43*, pp. 477-486.

KAYALAR, L. (1969) "Experimentelle und theoretische Untersuchungen uber den Einfluß des Turbulenzgrades auf den Warmeubergang in der Umgebung des Staupunktes eines Kreiszylinders", *Forschung auf dem Gebiete des Ingenieurwesens, 35*, pp. 157-167. [In German]

KESTIN, J., MAEDER, P.F. and SOGIN, H.H. (1961) "The Influence of Turbulence on the Transfer of Heat to Cylinders Near the Stagnation Point", *Zeitschrift fur Angewandte Mathmatik und Physik, 12*, pp. 115-132.

KESTIN, J., and WOOD, R.T. (1971) "The Influence of Turbulence on Mass Transfer from Cylinders", *Journal of Heat Transfer, 93*, pp. 321-327. Also: ASME Paper 70-WA/HT-3.

KWON, O.K., TURNER, E.R., and KOU, Y.M., 1983, "Prediction of Stagnation Flow Heat Transfer on Turbomachinery Airfoils," AIAA Paper No. 83-1173.

LIGHTHILL, M.J. (1954) "The Response of Laminar Skin Friction and Heat Transfer to Fluctuations in the Stream Velocity", *Proceedings of the Royal Society of London, Series A, 224*, pp. 1-23.

LIN, C.C. (1957) "Motion in the Boundary Layer with a Rapidly Oscillating External Flow", *Proceedings of the Ninth International Congress on Applied Mechanics, 4*, pp. 155-167.

LOWERY, G.W., and VACHON, R.I., (1975) "The Effect of Turbulence on Heat Transfer from Heated Cylinders", *International Journal Heat and Mass Transfer, 18*, pp. 1229-1224.

PAXSON, D.E., and MAYLE, R.E. (1991) "Laminar Boundary Layer Interaction With an Unsteady Passing Wake", *Journal of Turbomachinery, 113*, pp. 419-427.

SEBAN, R.A. (1960) "The Influence of Free Stream Turbulence on the Local Heat Transfer from Cylinders", *Journal of Heat Transfer, 82*, pp. 101-107.

SIKMANOVIC, S., OKA, S., and KONCAR-DJURDJEVIC, S. (1974) "Influence of the Structure of Turbulent Flow on Heat Transfer from a Single Cylinder in a Cross Flow", FC8.6, *Heat Transfer 1974: Proceedings of the Fifth International Heat Transfer Conference, Tokyo, Japan 1974, 2*, Hemisphere Publishing Corporation, Washington, D.C., pp. 320-324.

SMITH, M.C., and KUETHE, A.M. (1966) "Effects of Turbulence on Laminar Skin Friction and Heat Transfer", *The Physics of Fluids, 9*. pp. 2337-2344.

SOGIN, H.H. and SUBRAMANIAN, V.S. (1961) "Local Mass Transfer from Circular Cylinders in Cross Flow", *Journal of Heat Transfer, 83*, pp. 483-493.

TAULBEE, D.B. and TRAN, L. (1988) "Stagnation Streamline Turbulence", *AIAA Journal, 26*, pp. 1011-1013.

VAN DRESAR, N.T., and MAYLE, R.E. (1988) "Stagnation Transfer Rates for Incident Flow with High Turbulence Intensities", *Symposium on Fundamentals of Forced Convection Heat Transfer, HTD, 101*, ASME, New York, New York, pp. 165-172.

YARDI, N.R., and SUKHATME, S.P. (1978) "Effects of Turbulence Intensity and Integral Length Scale of a Turbulent Free Stream on Forced Convection Heat Transfer from a Circular Cylinder in Crossflow", FC(b)-29, *Proceedings of the Sixth International Heat Transfer Conference, Toronto, Canada 1978*. Hemisphere Publishing Company, Incorporated, Washington, D.C., pp. 347-352.

ZAPP, G.M.(1950) "The Effect of Turbulence on Local Heat Transfer Coefficients Around a Cylinder Normal to an Air Stream", M.S. Thesis, Oregon State University, Corvallis, Oregon.